

1 ***Non-IG::MYC* in diffuse large B-cell lymphoma confers variable genomic configurations and *MYC***
2 **transactivation potential**

3 Chunye Zhang^{1,2,*}, Ellen Stelloo^{3,*}, Sharon Barrans^{4,*}, Francesco Cucco^{1,5,*}, Dan Jiang^{1,6}, Maria-Myrsini
4 Tzioni¹, Zi Chen¹, Yan Li^{1,7}, Joost F Swennenhuis³, Jasmine Makker¹, Livia Rásó-Barnett⁸, Hongxiang
5 Liu⁶, Hesham El-Daly⁹, Elizabeth Soilleux¹, Nimish Shah¹⁰, Sateesh Kumar Nagumantry¹¹, Maw Kyaw¹²,
6 Mahesh Panatt Prahladan¹³, Reuben Tooze^{4,14}, David R. Westhead¹⁵, Harma Feitsma³, Andrew J
7 Davies¹⁶, Catherine Burton⁴, Peter W M Johnson¹⁶, Ming-Qing Du^{1,#}

8 *These authors contributed equally.

9

10 ¹Division of Cellular and Molecular Pathology, Department of Pathology, University of Cambridge,
11 Cambridge, UK;

12 ²Department of Oral Pathology, Shanghai Ninth People's Hospital, Shanghai Jiao Tong University
13 School of Medicine, Shanghai, PR China;

14 ³Cergentis BV, Utrecht, Netherlands;

15 ⁴Haematological Malignancy Diagnostic Service, St James' University Hospital, Leeds, UK;

16 ⁵Institute of Clinical Physiology, CNR, Pisa, Italy;

17 ⁶East Genomic Laboratory Hub, Cambridge University Hospitals NHS Foundation Trust, Cambridge,
18 UK;

19 ⁷Department of Haematology, Hebei General Hospital, Shijiazhuang, PR China;

20 ⁸The Haematopathology and Oncology Diagnostic Service, Cambridge University Hospitals NHS
21 Foundation Trust, Cambridge, UK;

22 ⁹Cellular Pathology Department, University Hospitals Coventry and Warwickshire NHS Trust,
23 Coventry, UK;

24 ¹⁰Department of Haematology, Norfolk and Norwich University Foundation Hospital;

25 ¹¹Department of Haematology, Peterborough City Hospital, Peterborough, UK;

26 ¹²Department of Haematology, James Paget University Hospitals NHS Foundation Trust, Great
27 Yarmouth, UK;

28 ¹³East Suffolk and North Essex Foundation Trust, Suffolk, UK;

29 ¹⁴Division of Haematology and Immunology, Leeds Institute of Medical Research, University of Leeds,
30 Leeds, UK.

31 ¹⁵School of Molecular and Cellular Biology, Faculty of Biological Sciences, University of Leeds, Leeds,
32 UK;

33 ¹⁶Cancer Research UK Centre and Southampton Clinical Trials Unit, University of Southampton,
34 Southampton, UK;

35

36 **Running title:** *Non-IG::MYC* in diffuse large B-cell lymphoma

37 **Key words:** DLBCL, *MYC* translocation partner, genomic configuration, transactivation

38 **Word Count:** Abstract: 200; the main manuscript text: 3468

39 **Manuscript figure and tables:** 7 Figures, 1 Table, 1 Supplementary Figure, 1 Supplementary
40 Table

41

42 **#Correspondence to:** Professor Ming-Qing Du, Division of Cellular and Molecular Pathology,
43 Department of Pathology, University of Cambridge, Level 3 Lab Block, Box231, Addenbrooke' s
44 Hospital, Hills Road, Cambridge, CB2 0QQ, UK.

45 Tel: +44 (0)1223 767092; Fax: +44 (0)1223 586670; Email: mqd20@cam.ac.uk

46 **Sources of Research support:** The research was supported by grants from Blood Cancer UK (19010,
47 19011) UK and Cancer Research UK (C8333/A29707), MMT was supported by a BBSRC DTP PhD
48 studentship (BBSRC BB/M011194/1). The Human Research Tissue Bank is supported by the NIHR
49 Cambridge Biomedical Research Centre.

50 **ABSTRACT**

51 *MYC* translocation occurs in 8-14% of diffuse large B-cell lymphoma (DLBCL), and may concur with
52 *BCL2* and/or *BCL6* translocation, known as double-hit (DH) or triple-hit (TH). DLBCL-*MYC/BCL2*-
53 DH/TH are largely germinal centre B-cell like subtype, but show variable clinical outcome, with
54 *IG::MYC* fusion significantly associated with inferior survival. While DLBCL-*MYC/BCL6*-DH are variable
55 in their cell-of-origin subtypes and clinical outcome. Intriguingly, only 40-50% of DLBCL with *MYC*
56 translocation show high *MYC* protein expression (>70%). We studied 186 DLBCLs with *MYC*
57 translocation including 32 *MYC/BCL2/BCL6*-TH, 75 *MYC/BCL2*-DH and 26 *MYC/BCL6*-DH. FISH
58 revealed a *MYC/BCL6* fusion in 59% of DLBCL-*MYC/BCL2/BCL6*-TH and 27% of DLBCL-*MYC/BCL6*-DH.
59 Targeted NGS showed a similar mutation profile and LymphGen genetic subtype between DLBCL-
60 *MYC/BCL2/BCL6*-TH and DLBCL-*MYC/BCL2*-DH, but variable LymphGen subtypes among DLBCL-
61 *MYC/BCL6*-DH. *MYC* protein expression is uniformly high in DLBCL with *IG::MYC*, but variable in
62 those with non-*IG::MYC* including *MYC/BCL6*-fusion. Translocation breakpoint analyses of 8 cases by
63 TLC-based NGS showed no obvious genomic configuration that enables *MYC* transactivation in 3 of
64 the 4 cases with non-*IG::MYC*, while a typical promoter substitution or *IGH* super enhancer
65 juxtaposition in the remaining cases. The findings potentially explain variable *MYC* expression in
66 DLBCL with *MYC* translocation, and also bear practical implications in its routine assessment.

67

68 INTRODUCTION

69 Diffuse large B-cell lymphoma (DLBCL) is a group of heterogeneous aggressive B-cell lymphoma with
70 variable cell-of-origin (COO), genetic changes, molecular mechanisms and clinical outcomes. Based
71 on COO, DLBCL can be broadly classified into activated B-cell like (ABC) and germinal centre B-cell
72 like (GCB) subtype, with a subset of the latter further identified as molecular high grade
73 (MHG)/double-hit signature (DHITsig) due to their enriched *MYC* expression and centromere
74 signatures [1,2]. Based on genetic alterations, DLBCL can be subdivided into distinct subgroups using
75 LymphGen algorithm or other: MCD (*MYD88*^{L265P} and *CD79B* mutations), N1 (*NOTCH1* mutation),
76 A53 (aneuploidy with *TP53* inactivation), BN2 (*BCL6* translocation and *NOTCH2* mutation), ST2 (*SGK1*
77 and *TET2* mutated) and EZB (*EZH2* mutation and *BCL2* translocation), with the latter subgroup
78 further divided into EZB-MYC+ and EZB-MYC- according to *MYC* signature [3,4]. There is a broad
79 correlation between COO molecular subtypes and genetic subgroups. ABC-DLBCL largely comprises
80 of MCD, N1 and A53, while GCB-DLBCL is primarily composed of EZB and ST2, with BN2 seen in both
81 ABC and GCB-DLBCL. These subgroups are further underpinned by their distinct molecular
82 mechanisms and different clinical outcomes.

83

84 Despite the steady progress in molecular characterization and sub-classification of DLBCL, few of
85 these advances are applied in a routine clinical setting. For routine diagnosis and prognostication of
86 DLBCL, only *MYC*, *BCL2* and *BCL6* translocations are investigated along with international prognostic
87 index. *MYC* translocation occurs in 8-14% of DLBCL. This translocation can occur together with *BCL2*
88 and/or *BCL6* translocation, known as double-hit (DH) or triple-hit (TH). Among *MYC* translocation
89 positive DLBCL, ~9% are *MYC/BCL2/BCL6*-TH, ~40% and ~18% are *MYC/BCL2*-DH and *MYC/BCL6*-DH
90 respectively [5-7]. Most of cases with *MYC/BCL2*-DH/TH are GCB subtype or EZB-MYC+ [3,5]. In
91 contrast, those with *MYC/BCL6*-DH are rather heterogeneous in their molecular subtypes, with 30%
92 each being GCB or ABC subtype respectively, 15% due to MHG, and the remaining cases

93 unclassifiable [5]. These cases showed a mutation profile remarkably different from those with
94 *MYC/BCL2*-DH/TH, but do not exhibit any prominent signatures although a proportion of these cases
95 are associated with *NOTCH2* mutation, thus BN2 subtype [5]. For these reasons, the 5th edition of
96 the World Health Organization Classification of Haematolymphoid Tumours (WHO-HAEM5) excludes
97 the cases with concomitant *MYC* and *BCL6* rearrangements (without *BCL2* rearrangement) from the
98 DH entity and renames the entity as diffuse large B-cell lymphoma/high-grade B-cell lymphoma with
99 *MYC* and *BCL2* rearrangements (DLBCL/HGBL-*MYC/BCL2*) to recognise their variable morphology [8].

100

101 The clinical outcome of DLBCL/HGBL-*MYC/BCL2*-DH is also heterogeneous. Cases with *IG::MYC* are
102 significantly associated with worse progression-free survival (PFS) and overall survival (OS),
103 particularly within the first two years of diagnosis, while those with non-*IG::MYC* showed no
104 significant difference in both PFS and OS from DLBCL without *MYC* translocation [7,9]. The
105 molecular mechanisms underlying the different clinical impacts by *MYC* translocation partner are
106 unclear. In addition, *MYC* protein expression varies considerably in DLBCL with *MYC* translocation,
107 ranging from negative to 100% positivity in lymphoma cells [10-12]. In DLBCL with *IGH::MYC*, the
108 breakpoint commonly occurs in region spanning the 5'UTR and intron 1 of the *MYC* gene and the
109 switch region of the *IGH* locus respectively, thus placing the *MYC* gene in close proximity of the
110 highly active *IGH* super enhancer, causing *MYC* constitutive over-expression [13]. Moreover, DLBCL
111 with *IGH::MYC* often acquire *MYC* mutations that impair *MYC* protein degradation, consequently
112 sustaining its expression and function [5]. However, the impact of non-*IG* partner on *MYC*
113 expression is unclear. Among the known non-*IG* partners of *MYC* translocation including *BCL6*,
114 *ZCCHC7* and *RFTN1*, *BCL6* is the most frequent [13,14]. It also remains unclear how often non-
115 *IG::MYC* translocation involves *BCL6* as a partner, and how non-*IG::MYC* impacts on *MYC* activation
116 given their clear difference in clinical impact from the *IG::MYC* translocation. To investigate these,
117 we studied 186 cases of DLBCL with *MYC* translocation including 32 *MYC/BCL2/BCL6*-TH, 75

118 *MYC/BCL2*-DH and 26 *MYC/BCL6*-DH by combined analyses of *MYC* translocation partner and *MYC*
119 protein expression, mutation profiling and breakpoint analysis of *MYC* translocation in selected cases
120 to understand their transactivation potential.

121

122 **MATERIALS AND METHODS**

123 The study was performed in accordance with local ethical guidelines for the research use of tissue
124 materials with the approval of the ethics committees of the involved institutions (05-Q1604-10, 04-
125 Q1205-125, 10-H0504-79).

126

127 A total of 186 cases of DLBCL with *MYC* translocation were retrieved from surgical files of
128 Addenbrookes Hospital, University of Cambridge and HMDS, St James' University Hospital, Leeds,
129 UK. These cases comprised of 32 *MYC/BCL2/BCL6*-TH, 75 *MYC/BCL2*-DH, 26 cases with *MYC/BCL6*-
130 DH, and 53 cases *MYC*-single hit (SH) (Figure 1).

131

132 **Interphase fluorescence in situ hybridisation (FISH)**

133 Chromosome translocation status at the *MYC*, *BCL2* and *BCL6* locus was available from routine
134 haematopathological diagnosis or previous studies [5]. Further interphase FISH with *MYC/BCL6*
135 (Cytocell), *MYC/IGH* (Abbott), *MYC/IGK* and *MYC/IGL* (Cytocell) dual fusion probes were performed on
136 FFPE tissue slides where indicated in the present study.

137

138 **Immunohistochemistry**

139 MYC (Abcam clone Y69) and BCL6 (Leica Clone LN22) immunohistochemistry were performed where
140 possible in all cases where tissue materials remained available using the Bond-III system (Leica
141 Biosystems) with the Bond Polymer Refine Detection Kit as the same condition of routine
142 histopathological diagnosis. This was carried out centrally in the Cambridge lab and the staining
143 intensity (weak, moderate, strong) and percentage in tumour cells (>70% or <70%) were scored [11].

144

145 **DNA extraction and quality assessment.**

146 Histology was reviewed and areas containing confluent lymphoma cells (>40%) in each specimen
147 were microdissected on consecutive tissue sections. DNA was extracted using the QIAamp DNA
148 Micro Kit (QIAGEN, Crawley, UK), quantified with a Qubit® Fluorometer (Life Technologies, UK) and
149 assessed for quality by PCR [5,15].

150

151 **Mutation analysis by targeted sequencing**

152 The mutation data in 125 cases were from a previous study, in which a panel of B-cell lymphoma
153 associated genes (n=70) were sequenced using HaloPlexHS target enrichment and Illumina
154 HiSeq4000 platform, with a well-validated in house variant calling pipeline [5]. In 53 cases,
155 mutation data were similarly obtained but using TWIST capture target enrichment of a much larger
156 gene panel (n=191) (Table S1) [16].

157 LymphGen genetic subtypes were assigned where possible according to Wright et al [3].

158

159 **Targeted locus capture next generation sequencing (TLC-NGS)**

160 TLC-NGS was essentially carried out as previously described [17]. FFPE tissue sections were
161 deparaffinised, followed by a 30 minute pretreatment step at 90°C, digestion with NlaIII restriction
162 enzyme and ligation with T4 DNA ligase. The sample was incubated at 80°C overnight to reverse

163 crosslinking and then subjected to DNA purification. A total of 100ng DNA was fragmented and used
164 for NGS library preparation, hybridization with capture probes using Roche HyperCap reagents
165 according to the manufacturer's instructions. Paired-end sequencing was performed using an
166 Illumina Novaseq 6000. TLC-NGS reads were mapped to the human genome (hg19) using BWA-
167 MEM (version: 0.7.17-r1188; settings: -SP -k12 -A2 -B3) in paired-end mode, and gene
168 rearrangements were identified using PLIER (Proximity-Ligation based Identification of
169 Rearrangements) according to previously validated pipeline [17].

170

171 **Statistical analysis:** Associations among *MYC* translocation, translocation partner and *MYC* protein
172 expression were analysed using the Fisher's exact test. All quoted *P* values are two-sided.

173

174 **RESULTS**

175 ***BCL6* frequently involves *MYC* translocation in DLBCL with *MYC/BCL6/BCL2*-TH or *MYC/BCL6*-DH**

176 Interphase FISH with the *BCL6/MYC* fusion probe was performed in 54 cases of DLBCL with
177 *MYC/BCL2/BCL6*-TH (n=32) or *MYC/BCL6*-DH (n=22). Among these cases, 25 (46.3%) had evidence of
178 genomic fusion between the *MYC* and *BCL6* loci by FISH (Figure 2A), and the frequency of *MYC/BCL6*
179 fusion was significantly higher in the *MYC/BCL2/BCL6*-TH (19/32=59%) than the *MYC/BCL6*-DH
180 (6/22=27%) group (Figure 2B).

181

182 Among the 25 cases with FISH evidence of *MYC/BCL6* fusion, 24 had complete data on *IG/MYC*
183 fusion by interphase FISH with the *MYC/IGH* fusion probe, and additional *MYC/IGK(L)* fusion probe if
184 no evidence of *MYC/IGH* fusion. Six of these cases had an *IGH::MYC* fusion, and this is consistent
185 with previous observation of a three way translocation involving the *MYC*, *BCL6* and *IGH* loci by
186 cytogenetic studies [18].

187

188 **Genetic features of DLBCL with *MYC/BCL6* fusion**

189 Mutation profiling by targeted NGS was carried out in 178 cases, and 135 of these cases were
190 successfully subtyped using the LymphGen algorithm [3].

191 Overall, the mutation profile of the *MYC/BCL2/BCL6*-TH group is very similar to that of the
192 *MYC/BCL2*-DH group (Figure 3A), characterised by frequent mutations in follicular lymphoma
193 associated genes (*BCL2*, *CREBBP*, *KMT2D*, *EZH2*, *TNFRSF14*). Our previous study shows that most
194 cases with *MYC/BCL2/BCL6*-TH, like those with *MYC/BCL2*-DH, are GCB, with a subset being MHG [5].
195 In support of this, the present study further demonstrated that both *MYC/BCL2/BCL6*-TH
196 (22/24=92%) and *MYC/BCL2*-DH (65/67=97%) groups were predominantly the EZB-MYC+ genetic
197 subtype. Within the *MYC/BCL2/BCL6*-TH group, there were no apparent differences in the mutation
198 profile and LymphGen genetic subtype between *MYC/BCL6* fusion positive and negative cases
199 (Figure 3A).

200

201 In contrast, the mutation profile of DLBCL-*MYC/BCL6*-DH was of less characteristic, but clearly
202 differed from that of the *MYC/BCL2/BCL6*-TH or *MYC/BCL2*-DH group (Figure 3A). The *MYC/BCL6*-DH
203 cases vary in their COO subtype as shown in our previous study [5]. The present study further
204 demonstrated that these cases varied in their LymphGen genetic subtypes although more frequently
205 being the BN2 subtype or unclassifiable (Figure 3B). Within the *MYC/BCL6*-DH group, there were
206 also no apparent differences in the mutation profile and genetic subtype between *MYC/BCL6* fusion
207 positive and negative cases albeit based on few cases.

208

209 **MYC protein expression is uniformly high in cases with *IG::MYC* but varies in those with non-**

210 ***IG::MYC***

211 Given that *MYC* translocation is thought to dysregulate its transcription control, we compared *MYC*
212 protein expression according to *MYC* translocation partner. High *MYC* expression was defined when
213 the protein is expressed in 70% of lymphoma cells with moderate to strong staining by
214 immunohistochemistry as such high *MYC* protein expression has been previously shown to identify
215 high risk cases [11].

216

217 High *MYC* protein expression was seen in each of the 20 cases of DLBCL with *IG::MYC* translocation
218 investigated (Figure 4). Among DLBCL with non-*IG::MYC* translocation including those with
219 *MYC/BCL6* fusion, *MYC* expression was variable, with only up to 50% cases showing a high *MYC*
220 protein expression (Figure 4B). There was no difference in the proportion of cases with high *MYC*
221 protein expression between the *MYC/BCL6* fusion positive and negative groups (Figure 4). These
222 findings suggest that non-*IG::MYC* translocations may have variable effects on *MYC* transcription
223 control and not every non-*IG::MYC* translocation can cause constitutive *MYC* expression.

224

225 **Breakpoint analysis of *MYC* translocation reveal insights explaining variable *MYC* expression**

226 To investigate why *MYC* protein expression was variable in cases with non-*IG::MYC* translocation, we
227 performed TLC-NGS and breakpoint analyses in 8 cases, including 4 with non-*IG::MYC* (3 with
228 *MYC/BCL6* fusion) and 4 with *IGH::MYC* respectively. In each case, TLC-NGS investigation confirmed
229 the findings of FISH analyses, and importantly unravelled the breakpoints and orientation of the
230 involved genes, thus helping to understand their transcriptional potential (Table 1).

231

232 Among the three cases with *MYC/BCL6* fusion, two (DLBCL-134, DLBCL-173) involved direct
233 juxtaposition between the *MYC* and *BCL6* loci, with the breakpoints occurring downstream or at the
234 3'UTR of the *MYC* gene, but upstream or within the intron 1 of the *BCL6* gene (Figure 5). In both

235 cases, the rearranged *MYC* and *BCL6* genes were in an opposite orientation, thus no structural
236 changes in the 5' region of *MYC* transcriptional control albeit uncertain on any potential effect of the
237 super enhancers downstream of the *MYC* and also at the 5' region of the *BCL6* gene [19,20]. In both
238 cases, the *MYC* protein expression was weak in <40% lymphoma cells. In the remaining case with
239 *MYC/BCL6* fusion (DLBCL-123), an insertion of a segment of chromosome 3 sequence neighbouring
240 to the *BCL6* locus together with a segment of the *IGH* switch region occurred within the intron 1 of
241 the *MYC* gene (Figure 6). Although the precise breakpoints of the inserted *IGH* sequence could not
242 be accurately defined, the involved region spanned the switch super enhancer, which could
243 potentially drive *MYC* expression. In keeping with this, *MYC* protein was strongly expressed in most
244 lymphoma cells in this case (Figure 6).

245

246 Among the 5 cases without *MYC/BCL6* fusion by FISH, TLC-NGS analyses confirmed the FISH
247 observations in each case, and further identified their translocation partners (Table 1). Two cases
248 showed a novel *MYC* translocation: one fused with *TOX* at 8q12 in an opposite orientation (DLBCL-
249 136), the other fused with *HNRNPA1* at 12q13 in the same orientation (DLBCL-154) (Figure 5-6). In
250 both cases, the *MYC* breakpoint occurred either upstream (in the case with *TOX*) or in the intron 1
251 (in the case with *HNRNPA1*) of the *MYC* gene. In the case of *TOX/MYC* fusion, *MYC* transcription was
252 unlikely driven directly by the *TOX* gene as the translocated *TOX* was in opposite orientation with
253 *MYC* and loose its 5' transcriptional regulatory region, but *MYC* protein expression was moderately
254 high. Interestingly, both TLC-NGS and interphase FISH in this case showed increased copies of both
255 the rearranged (3-6 copies by interphase FISH) and non-rearranged (2 copies by interphase FISH)
256 *MYC* alleles, in keeping with the variable staining extensity among lymphoma cells (Figure 5, Figure
257 S1). In the case with *HNRNPA1::MYC* fusion, *MYC* was in the same orientation with *HNRNPA1*, and
258 placed under the transcription control of *HNRNPA1*. *HNRNPA1* encodes a heterogeneous nuclear

259 ribonucleoprotein that is ubiquitously expressed, and strong *MYC* protein expression was uniformly
260 seen in lymphoma cells of this case (Figure 6).

261 In the remaining three cases (L0318, DLBCL-96, DLBCL-178) without *MYC/BCL6* fusion, *MYC*
262 translocation was associated with *IGH* (Table 1).

263

264 Apart from the above novel *MYC* translocations, TLC-NGS also identified previously known
265 *LCP1::BCL6* (DLBCL-178, Figure 7) and *CIITA::BCL6* fusion each in one case (DLBCL-136, Figure 5). In
266 both cases, the genomic fusion was in the same orientation and the breakpoint was in the intron 1
267 of both *BCL6* gene and its partner gene, and these genomic configurations are typical of *BCL6*
268 promoter substitution by its translocation which causes enhanced *BCL6* expression (Figure 5 and 7).

269 In the case with *HNRNPA1::MYC* fusion (DLBCL-154), TLC-NGS revealed additionally a complex fusion
270 among *BCL6*, *IGH* and *BCL2* (Figure 6), with the *IGH* segment (from the joining to the switch region)
271 in between the *BCL6* and *BCL2* gene on derivative chromosome 3. In this case, the presence of *IGH*
272 super enhancers (at both joining and switch region) most likely drive constitutive *BCL6* and *BCL2*
273 transactivation, hence the strong expression of both proteins in lymphoma cells (Figure 6).

274

275 **DISCUSSION**

276 The present study reports several significant novel findings, and they include: 1) *MYC* and *BCL6*
277 translocation in a significant proportion of DLBCL, particularly those with *MYC/BCL2/BCL6*-TH, are
278 due to a direct juxtaposition between the *MYC* and *BCL6* loci, rather than being an independent
279 event; 2) *MYC* protein expression is uniformly high in DLBCL with *IG::MYC*, but varies in those with
280 non-*IG::MYC*, including *BCL6/MYC* fusion; 3) *MYC* translocation with non-*IG* partner may not always
281 acquire a genomic configuration that enables *MYC* constitutive transactivation, resulting in high *MYC*

282 expression. These findings provide molecular insights, which explain several perplexing features of
283 DLBCL with *MYC* translocation, and also bear practical implications in routine prognostic assessment.

284

285 *MYC* and *BCL6* translocation detected by interphase FISH with their respective break-apart probes
286 was commonly referred as independent oncogenic events, thus recorded as DH or TH when
287 additional *BCL2* translocation is present. Remarkably, 59% of the so-called *MYC/BCL2/BCL6*-TH and
288 27% of *MYC/BCL6*-DH DLBCL are actually due to a direct genomic fusion between the *MYC* and *BCL6*
289 loci. The finding is not totally unexpected as *MYC* is one of the many promiscuous translocation
290 partners of *BCL6*, and $t(3;8)(q27;q24)/BCL6::MYC$ and $t(3;8;14)(q27;q24;q32)/IGH::BCL6/MYC$ have
291 been previously reported [18,21].

292

293 A major molecular mechanism underpinning the oncogenic potential of *MYC* translocation is its
294 transactivation due to juxtaposition to a super enhancer, such as those at the *IGH* joining and switch
295 region or promoter substitution. The *IGH* super enhancers are expected to be highly active in all
296 mature B-cells as they express high levels of immunoglobulin. Such super-enhancer mediated
297 transcriptional activation, unlike promoter substitution, is independent of the genomic orientation
298 of the *MYC* and *IG* genes and to a certain extent also of the “linear” distance between the two genes
299 [22], thus explaining the uniform high *MYC* protein expression seen in DLBCL with *IG::MYC*, and also
300 Burkitt lymphoma.

301

302 Among the 4 cases of DLBCL with non-*IG::MYC* investigated by TLC-NGS, 3 showed *MYC* gene in an
303 opposite orientation with its translocation partner (*BCL6*, *TOX*), without affecting the *MYC* promoter
304 region. The moderate variable *MYC* expression in the case with *TOX::MYC* (DLBCL-136) is most likely

305 the result of *MYC* gene amplification (Figure 5, Figure S1). Otherwise, there was no evidence of
306 constitutive *MYC* expression in these cases. There were potential super enhancers downstream of
307 the *MYC* gene and in the translocated *BCL6* region [19,20], the potential impact on these super
308 enhancers by these translocations is unclear. As the transactivation potential of super enhancers
309 depend on cell type and differentiation stage and is regulated by a range of factors, such as
310 genetic/epigenetic modifications and transcriptional factor binding [20,23,24], different
311 translocations may give rise to variable potentials of *MYC* transactivation, from low levels of
312 dysregulation to utmost constitutive activation. Nonetheless, lack of high *MYC* expression in these
313 cases suggests these translocations do not cause *MYC* constitutive transactivation. This speculation
314 is in keeping with the previous observation that a proportion of DLBCL with *MYC* translocation lack
315 high *MYC* mRNA and protein expression [11,12]. In contrast, the remaining case (DLBCL-154) with
316 *HNRNPA1::MYC* is a typical promoter substitution, and shows strong uniform *MYC* expression as
317 expected since *HNRNPA1*, encoding for an RNA binding protein, is ubiquitously expressed (Figure 6).

318

319 The above findings potentially explain why *IGH::MYC*, but not *non-IG::MYC* confers significantly
320 inferior survival in patients with DLBCL-*MYC/BCL2*-DH [7], and also why ~25% of DLBCL with *MYC*
321 translocation, including those with a *MYC/BCL2*-DH, are conventional GCB, but not MHG subtype [1].
322 Our observations also highlight the heterogeneous *MYC* expression in DLBCL with *non-IG::MYC*
323 translocation. Of note, 44% of DLBCL with *non-IG::MYC/BCL2*-DH lacked high *MYC* protein expression
324 above 70% (Figure 3A). It remains to be investigated whether there is any potential difference in
325 clinical outcome between *non-IG::MYC* translocation positive DLBCL with high and low *MYC* protein
326 expression, and whether those with high *MYC* expression are similar to cases with *IG::MYC* in their
327 clinical outcome. To address this pivotal question, a large cohort of genetic subtype matched DLBCL
328 with *MYC* translocation, such as those with *MYC/BCL2*-DH, is required.

329

330 In DLBCL, *MYC* and *BCL6* translocation are most likely acquired due to relentless exposure to somatic
331 hypermutation and class switch activities during B-cell expansion in germinal centres, and are likely a
332 secondary event [13,25]. This is particularly evident in cases with *BCL2* translocation, which is the
333 primary genetic event, occurring as a consequence of erroneous VDJ recombination at the pre-B
334 stage of B-cell development in the bone marrow. The secondary structural changes may not be
335 always a driver event, similar to the point mutations in many well-known lymphoma genes acquired
336 due to somatic hypermutation activities [26]. In view of this and the above discussion, it is pertinent
337 to question whether every non-*IG::MYC* translocation in DLBCL is an activation event, albeit to be
338 attested in future studies.

339

340 In routine clinical practice, interphase FISH is used for detection of *MYC*, *BCL2* and *BCL6*
341 translocation, together with their translocation partners, although commonly only including *IGH*.
342 Among *MYC* translocation positive DLBCL, *IG::MYC* accounts for ~55% of cases [7,9]. The full
343 spectrum of non-*IG* partners of *MYC* translocation remains to be characterised although *BCL6* may
344 account for a majority. A major challenge to delineate whether a non-*IG/MYC* translocation is a
345 constitutive activation event, thus clinically important, is to characterise its genomic configuration,
346 search for evidence that enables *MYC* constitutive transactivation. This cannot be resolved by
347 interphase FISH even when the translocation partner is known, but requires breakpoint analyses
348 such as by TLC-NGS which is not yet available in a routine clinical setting. In the absence of any
349 knowledge of genomic configuration of the translocation, the pathogenic potential and the
350 prognostic value of non-*IG/MYC* translocation need to be interpreted in conjunction with *MYC*
351 protein expression.

352

353 Our findings also raise the debate whether all DLBCL should be investigated for *MYC* translocation
354 with regard to risk stratification in routine histopathological diagnosis by interphase FISH or first
355 screened by *MYC* immunohistochemistry (where necessary immunohistochemistry with an
356 alternative antibody to rule out potential false negative due to mutation impairing the antibody
357 binding site [12]), and only cases with *MYC* protein expression above a certain level (to be
358 determined) selected for further FISH analyses. Further breakpoint analysis of non-*IG/MYC*
359 translocation and their correlation with the level of *MYC* protein expression in a large cohort should
360 help to resolve these practical issues. Nonetheless, it is important to routinely investigate whether
361 *MYC* translocation is associated with *IG* (both heavy and light chain) loci and *MYC* protein expression
362 as both have been shown to be associated with adverse clinical outcome.

363

364 In summary, a significant proportion of DLBCL with both *MYC* and *BCL6* translocations are due to
365 direct juxtaposition between the two genomic loci. *MYC* translocation involving non-*IG* loci including
366 *BCL6* varies in their genomic configurations, and may not often gain genomic configuration that can
367 cause constitute *MYC* transactivation, leading to its enhanced protein expression. The prognostic
368 value of *MYC* translocation needs to be interpreted in conjunction with its translocation partner and
369 *MYC* protein expression level.

370

371 **Acknowledgements:** The authors would like to thank Wanfeng Zhao for her help on
372 immunohistochemistry.

373

374 **Authors contributions:** FISH, targeted NGS, data collection and analyses: CZ, SB, FC, DJ, MMT, ZC,
375 YL, JM, MQD; TLC-NGS: ES, JFS, HF, MQD; FISH and pathology: LRB, HL, HED, ES, MQD; Clinical data:
376 NS, SKN, MK, MPP; Study design, case contribution, coordination and research funding: MQD, RT,

377 DRW, AJD, CB, PWMJ; Manuscript writing and preparation: MQD with contributions from all authors.

378 All authors read and approved the final manuscript.

379

380 **Conflict of interest:** ES, JFS and HF are employees of Cergentis, which owns patents on the TLC-NGS

381 method. The authors declare no conflict of interest.

382

383

384

385 **REFERENCES:**

- 386 1. Sha C, Barrans S, Cucco F, Bentley MA, Care MA, Cummin T *et al.* Molecular High-Grade
387 B-Cell Lymphoma: Defining a Poor-Risk Group That Requires Different Approaches to
388 Therapy. *J Clin Oncol.* 2019;37:202-12.
- 389 2. Ennishi D, Jiang A, Boyle M, Collinge B, Grande BM, Ben-Neriah S *et al.* Double-Hit Gene
390 Expression Signature Defines a Distinct Subgroup of Germinal Center B-Cell-Like Diffuse
391 Large B-Cell Lymphoma. *J Clin Oncol.* 2019;37:190-201.
- 392 3. Wright GW, Huang DW, Phelan JD, Coulibaly ZA, Roulland S, Young RM *et al.* A
393 Probabilistic Classification Tool for Genetic Subtypes of Diffuse Large B Cell Lymphoma
394 with Therapeutic Implications. *Cancer Cell.* 2020;37:551-68.e14.
- 395 4. Lacy SE, Barrans SL, Beer PA, Painter D, Smith AG, Roman E *et al.* Targeted sequencing
396 in DLBCL, molecular subtypes, and outcomes: a Haematological Malignancy Research
397 Network report. *Blood.* 2020;135:1759-71.
- 398 5. Cucco F, Barrans S, Sha C, Clipson A, Crouch S, Dobson R *et al.* Distinct genetic changes
399 reveal evolutionary history and heterogeneous molecular grade of DLBCL with
400 MYC/BCL2 double-hit. *Leukemia.* 2020;34:1329-41.
- 401 6. Clipson A, Barrans S, Zeng N, Crouch S, Grigoropoulos NF, Liu H *et al.* The prognosis of
402 MYC translocation positive diffuse large B-cell lymphoma depends on the second hit. *J*
403 *Pathol Clin Res.* 2015;1:125-33.
- 404 7. Rosenwald A, Bens S, Advani R, Barrans S, Copie-Bergman C, Elsensohn MH *et al.*
405 Prognostic Significance of MYC Rearrangement and Translocation Partner in Diffuse
406 Large B-Cell Lymphoma: A Study by the Lunenburg Lymphoma Biomarker Consortium. *J*
407 *Clin Oncol.* 2019;37:3359-68.

- 408 8. Alaggio R, Amador C, Anagnostopoulos I, Attygalle AD, Araujo IBO, Berti E *et al.* The 5th
409 edition of the World Health Organization Classification of Haematolymphoid Tumours:
410 Lymphoid Neoplasms. *Leukemia*. 2022;36:1720-48.
- 411 9. Copie-Bergman C, Cuillière-Dartigues P, Baia M, Briere J, Delarue R, Canioni D *et al.*
412 *MYC-IG* rearrangements are negative predictors of survival in DLBCL patients treated
413 with immunochemotherapy: a GELA/LYSA study. *Blood*. 2015;126:2466-74.
- 414 10. Ambrosio MR, Lazzi S, Bello GL, Santi R, Porro LD, de Santi MM *et al.* MYC protein
415 expression scoring and its impact on the prognosis of aggressive B-cell lymphoma
416 patients. *Haematologica*. 2019;104:e25-e8.
- 417 11. Ziepert M, Lazzi S, Santi R, Vergoni F, Granai M, Mancini V *et al.* A 70% cut-off for MYC
418 protein expression in diffuse large B cell lymphoma identifies a high-risk group of
419 patients. *Haematologica*. 2020;105:2667-70.
- 420 12. Collinge B, Ben-Neriah S, Chong L, Boyle M, Jiang A, Miyata-Takata T *et al.* The impact of
421 MYC and BCL2 structural variants in tumors of DLBCL morphology and mechanisms of
422 false-negative MYC IHC. *Blood*. 2021;137:2196-208.
- 423 13. Chong LC, Ben-Neriah S, Slack GW, Freeman C, Ennishi D, Mottok A *et al.* High-
424 resolution architecture and partner genes of MYC rearrangements in lymphoma with
425 DLBCL morphology. *Blood Adv*. 2018;2:2755-65.
- 426 14. Bertrand P, Bastard C, Maingonnat C, Jardin F, Maisonneuve C, Courel MN *et al.*
427 Mapping of *MYC* breakpoints in 8q24 rearrangements involving non-immunoglobulin
428 partners in B-cell lymphomas. *Leukemia*. 2007;21:515-23.
- 429 15. Wang M, Escudero-Ibarz L, Moody S, Zeng N, Clipson A, Huang Y *et al.* Somatic Mutation
430 Screening Using Archival Formalin-Fixed, Paraffin-Embedded Tissues by Fluidigm
431 Multiplex PCR and Illumina Sequencing. *J Mol Diagn*. 2015;17:521-32.

- 432 16. Tzioni MM, Wotherspoon A, Chen Z, Cucco F, Makker J, Du MQ. Divergent evolution of
433 metachronous follicular lymphoma and extranodal marginal zone lymphoma of
434 mucosa-associated lymphoid tissue from a common precursor. *J Pathol.* 2023;261:11-8.
- 435 17. Allahyar A, Pieterse M, Swennenhuis J, Los-de Vries GT, Yilmaz M, Leguit R *et al.* Robust
436 detection of translocations in lymphoma FFPE samples using targeted locus capture-
437 based sequencing. *Nat Commun.* 2021;12:3361.
- 438 18. De Paoli E, Bandiera L, Ravano E, Cesana C, Grillo G, Mancini V *et al.* A double-hit High-
439 grade B-cell lymphoma with three-way translocation t(3;8;14)(q27;q24;q32) involving
440 *BCL6*, *MYC*, and *IGH*. *Clin Case Rep.* 2018;6:2411-5.
- 441 19. Bahr C, von Paleske L, Uslu VV, Remeseiro S, Takayama N, Ng SW *et al.* A *Myc* enhancer
442 cluster regulates normal and leukaemic haematopoietic stem cell hierarchies. *Nature.*
443 2018;553:515-20.
- 444 20. Bal E, Kumar R, Hadigol M, Holmes AB, Hilton LK, Loh JW *et al.* Super-enhancer
445 hypermutation alters oncogene expression in B cell lymphoma. *Nature.* 2022;607:808-
446 15.
- 447 21. Johnson SM, Umakanthan JM, Yuan J, Fedoriw Y, Bociek RG, Kaiser-Rogers K *et al.*
448 Lymphomas with pseudo-double-hit *BCL6-MYC* translocations due to t(3;8)(q27;q24)
449 are associated with a germinal center immunophenotype, extranodal involvement, and
450 frequent *BCL2* translocations. *Hum Pathol.* 2018;80:192-200.
- 451 22. Pinaud E, Marquet M, Fiancette R, Péron S, Vincent-Fabert C, Denizot Y *et al.* The IgH
452 locus 3' regulatory region: pulling the strings from behind. *Adv Immunol.* 2011;110:27-
453 70.

- 454 23. Ryan RJ, Drier Y, Whitton H, Cotton MJ, Kaur J, Issner R *et al.* Detection of Enhancer-
455 Associated Rearrangements Reveals Mechanisms of Oncogene Dysregulation in B-cell
456 Lymphoma. *Cancer Discov.* 2015;5:1058-71.
- 457 24. Iyer AR, Gurumurthy A, Kodgule R, Aguilar AR, Saari T, Ramzan A *et al.* Selective
458 Enhancer Dependencies in *MYC* -Intact and *MYC* -Rearranged Germinal Center B-cell
459 Diffuse Large B-cell Lymphoma. *bioRxiv.* 2023.
- 460 25. Dobson R, Wotherspoon A, Liu SA, Cucco F, Chen Z, Tang Y *et al.* Widespread in situ
461 follicular neoplasia in patients who subsequently developed follicular lymphoma. *J*
462 *Pathol.* 2022;256:369-77.
- 463 26. Hübschmann D, Kleinheinz K, Wagener R, Bernhart SH, López C, Toprak UH *et al.*
464 Mutational mechanisms shaping the coding and noncoding genome of germinal center
465 derived B-cell lymphomas. *Leukemia.* 2021;35:2002-16.
- 466

467 **FIGURE LEGENDS**

468 **Figure 1:** Summary of DLBCL with MYC translocation and experiments carried out.

469

470 **Figure 2:** *MYC/BCL6* fusion accounts for a high proportion of DLBCL with *MYC* and *BCL6*

471 translocation. A: Example of interphase FISH in a case with a triple hit (TH), in which the *MYC* and

472 *BCL6* translocation detected by their breakapart probes (BAP) are due to *MYC/BCL6* fusion. B: The

473 frequency of *MYC/BCL6* fusion is significantly higher in cases with *MYC/BCL6/BCL2*-“TH” than those

474 with *MYC/BCL6* “double hit” (DH).

475

476 **Figure 3:** Mutation profile (A) and LymphGen genetic subtype (B) according to translocation status.

477 tr: translocation; IHC: immunohistochemistry; TH: triple hits; DH: double hits.

478

479 **Figure 4:** MYC protein expression and its correlation with MYC translocation partner.

480 A: examples of MYC immunohistochemistry and grading; B: High MYC protein expression is

481 invariably seen in DLBCL with *IG::MYC*, but only in up to 50% cases with non-*IG::MYC* translocation..

482

483 **Figure 5:** *MYC* translocation with *BCL6* or other partners lacks genomic configuration that activates

484 MYC transcription. Genomic breakpoint sequencing analyses was performed by targeted locus

485 capture-based next generation sequencing (TLC-NGS) with sequence annotations based on human

486 genome (hg19). E: exon (fill box: coding exon; non-filled box: non-coding exon). Cen: centromere;

487 Tel: telomere.

488

489 **Figure 6:** *MYC* translocation with *IGH* or novel partner confers genomic configuration that activates
490 *MYC* transcription. Genomic breakpoint sequencing analyses was performed by targeted locus
491 capture-based next generation sequencing (TLC-NGS) with sequence annotations based on human
492 genome (hg19).). E: exon (fill box: coding exon; non-filled box: non-coding exon). Cen: centromere;
493 Tel: telomere.

494

495 **Figure 7:** *MYC* translocation with *IGH* or novel partner confers genomic configuration that activates
496 *MYC* transcription. Genomic breakpoint sequencing analyses was performed by targeted locus
497 capture-based next generation sequencing (TLC-NGS) with sequence annotations based on human
498 genome (hg19).). E: exon (fill box: coding exon; non-filled box: non-coding exon). Cen: centromere;
499 Tel: telomere.

500

501 **Table 1.** Detection of chromosome translocation by TLC-NGS.

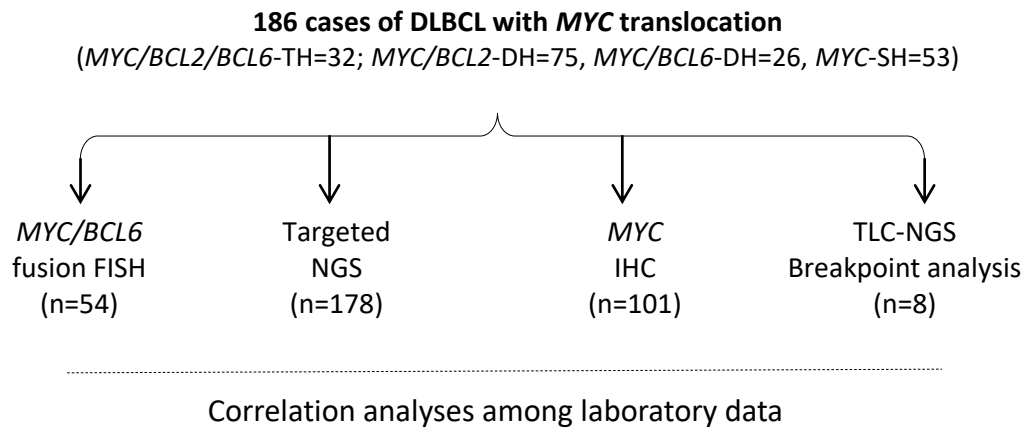


Figure 1

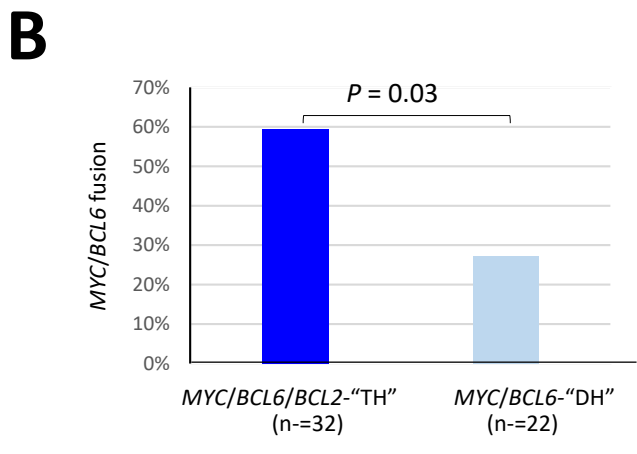
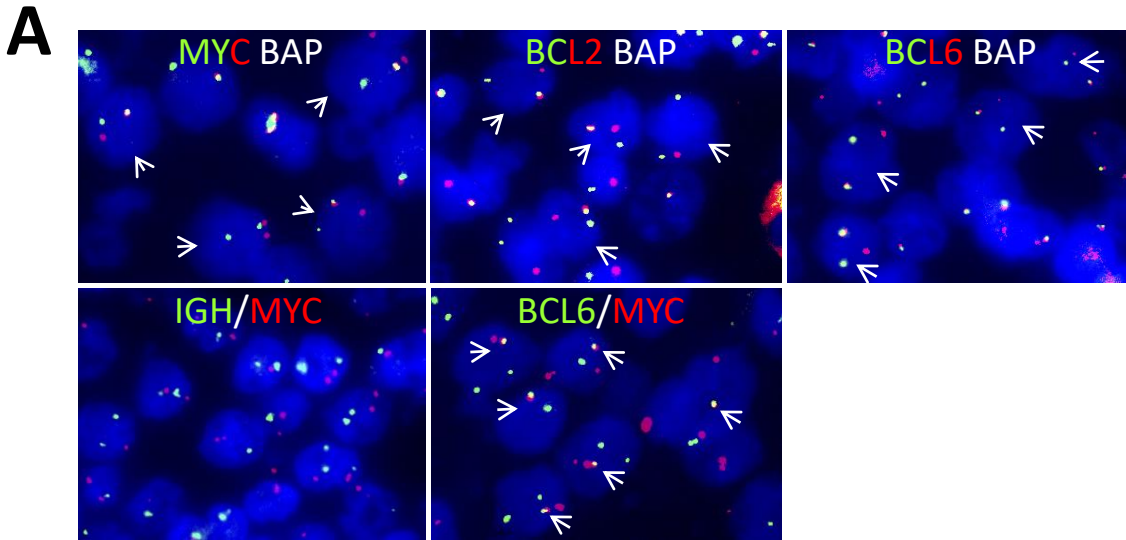
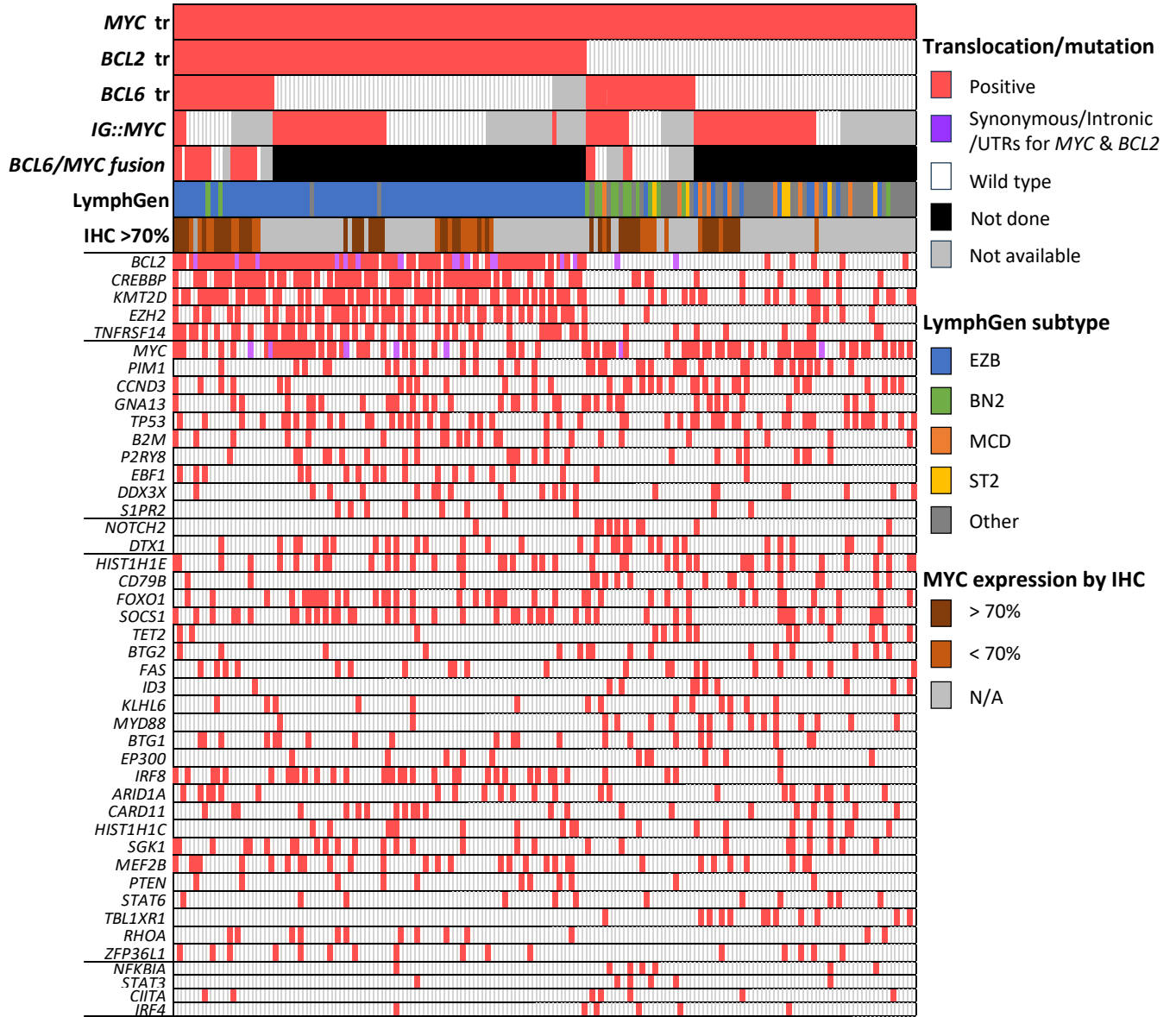


Figure 2

A



B

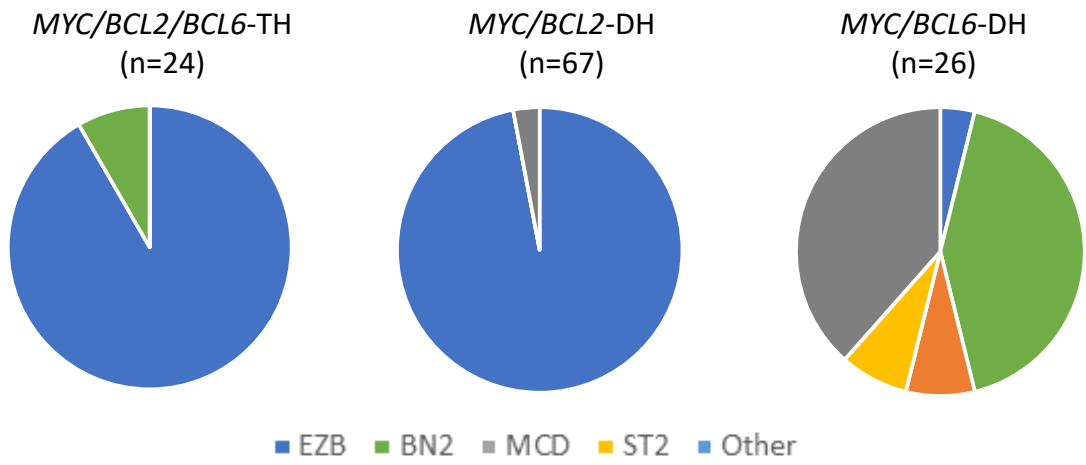


Figure 3:

A

Examples of MYC immunohistochemistry

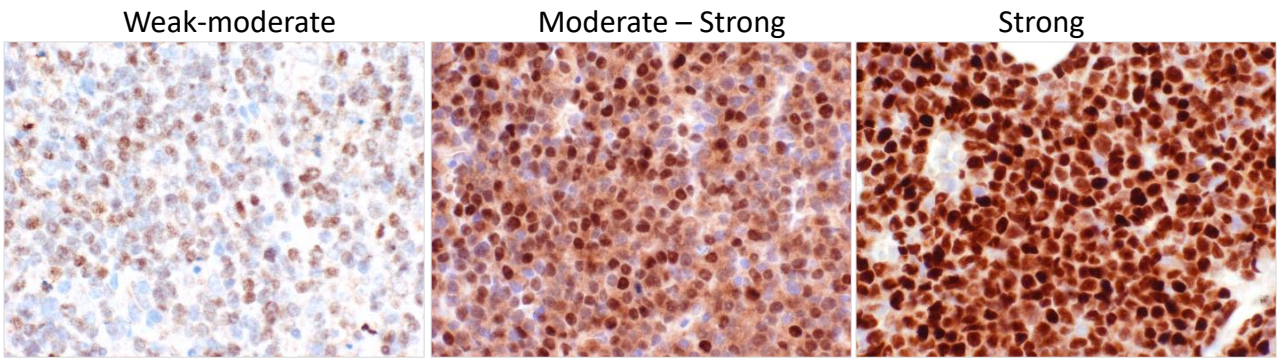
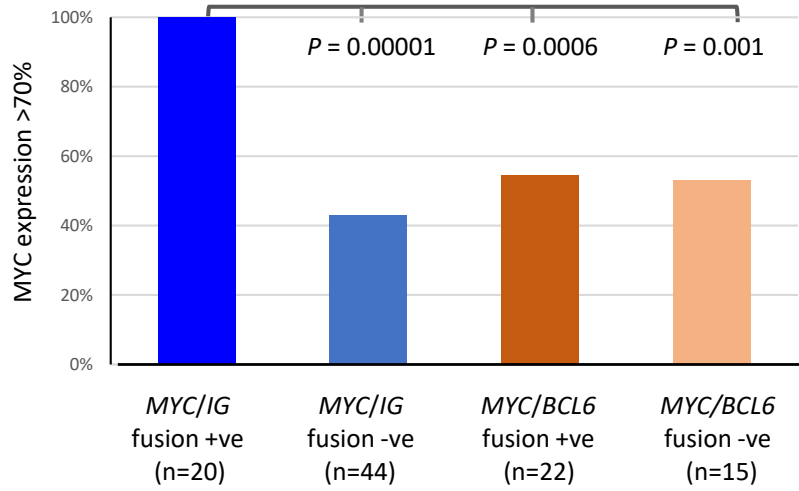
**B**

Figure 4

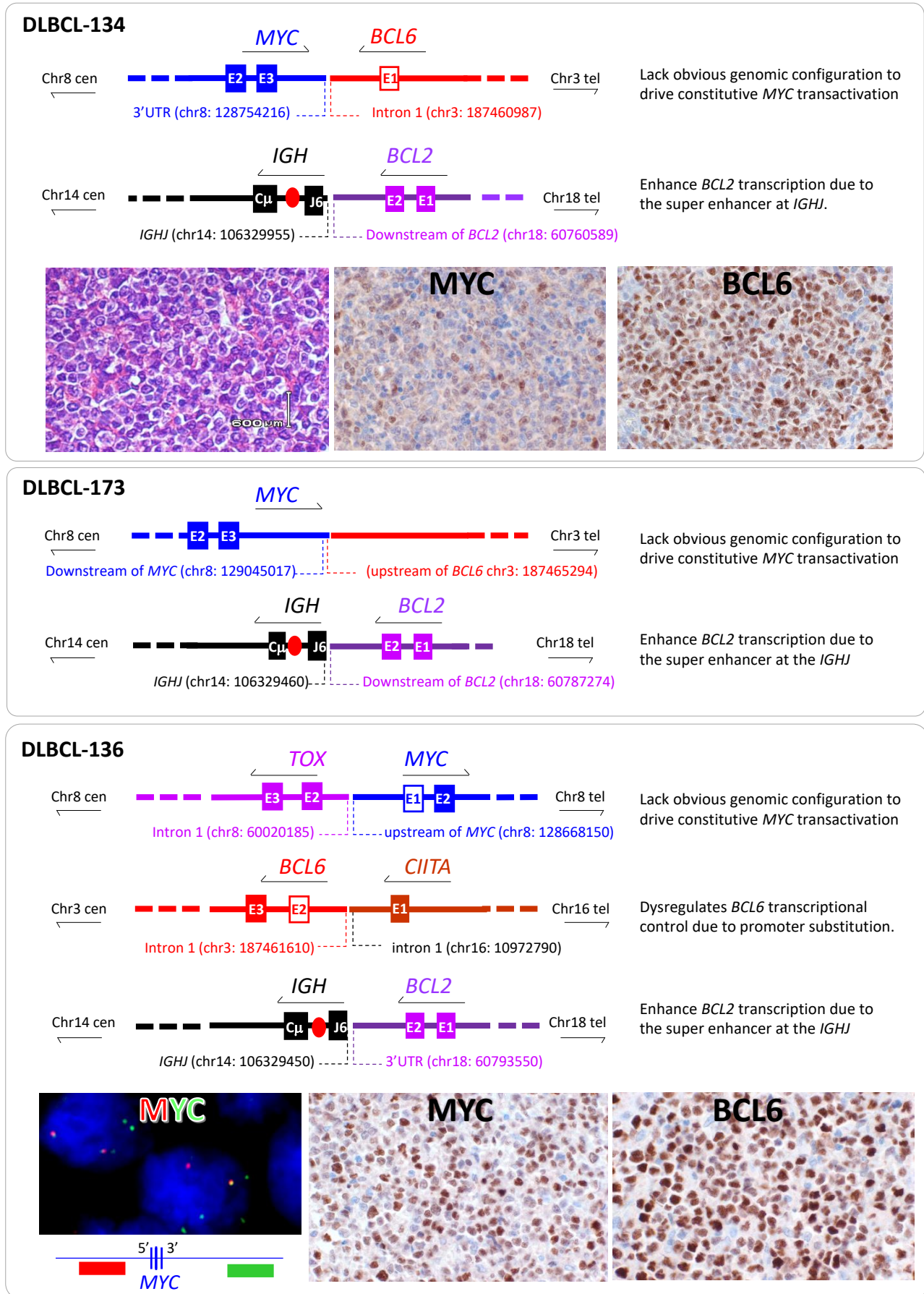
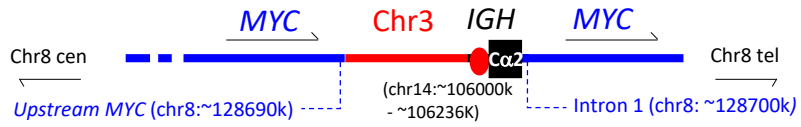
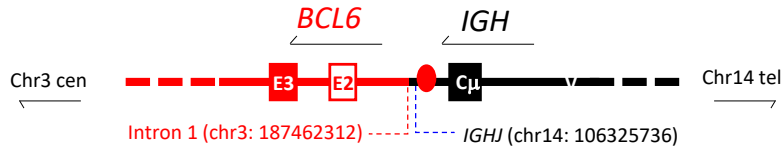


Figure 5

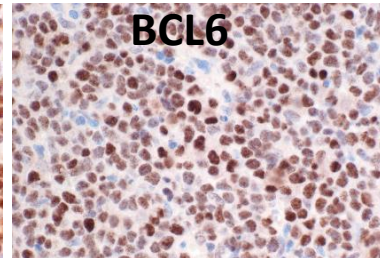
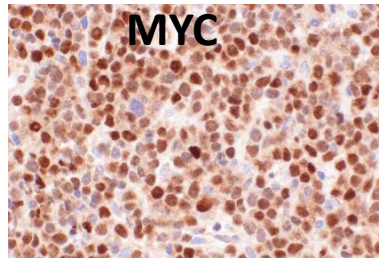
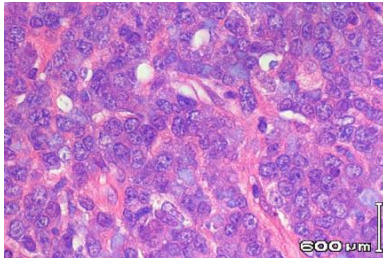
DLBCL-123



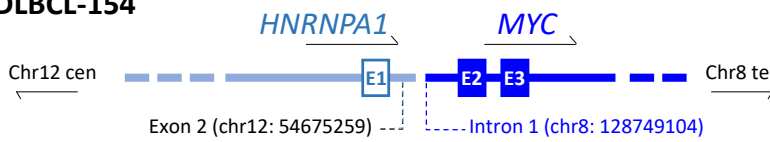
The fusion breakpoint could not be defined precisely, but *MYC* expression is likely dysregulated by *IGH* enhancer



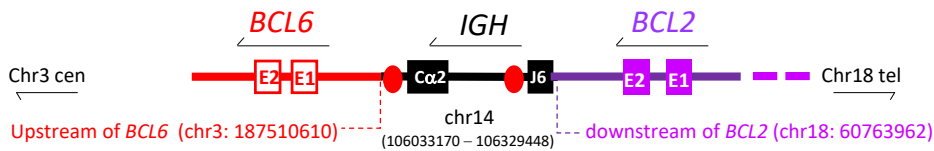
Enhance *BCL6* transcription due to the super enhancer at *IGHJ*.



DLBCL-154



Dysregulate *MYC* transcriptional control due to promoter substitution.



Enhance both *BCL2* and *BCL6* transcription due to *IGH* super enhancer

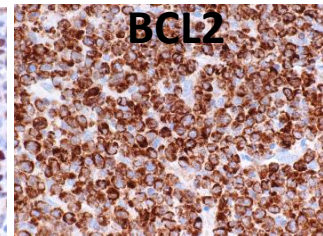
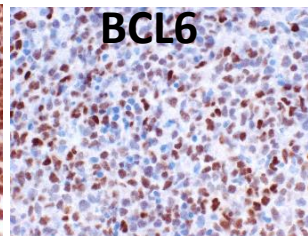
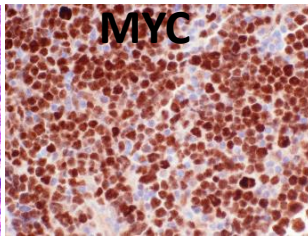
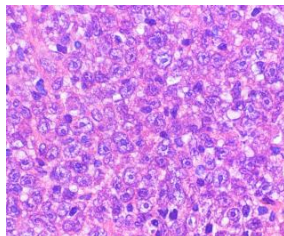


Figure 6

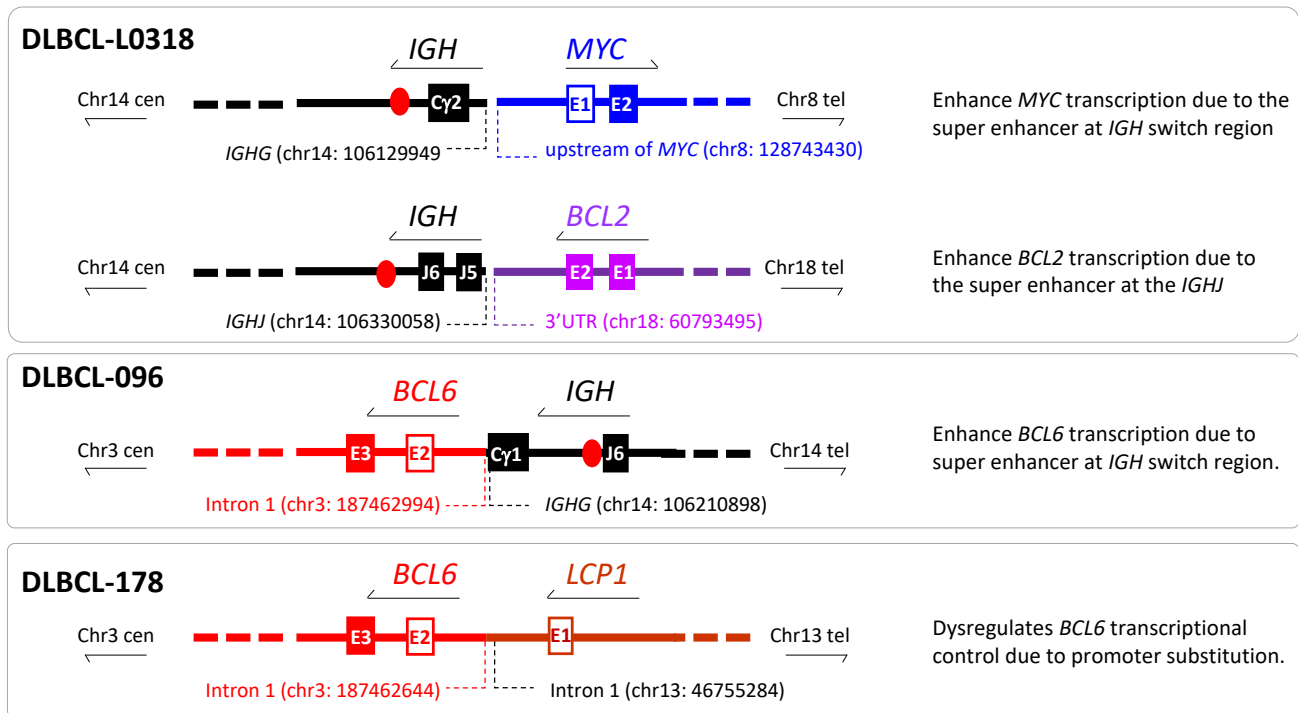


Figure 7

Table 1. Detection of chromosome translocation by TLC-NGS.

Targets* Case	BCL2	BCL6	MYC	IGH
DLBCL-134	<i>IGH</i>	MYC	<i>BCL6</i>	<i>BCL2</i>
DLBCL-173	<i>IGH</i>	MYC	<i>BCL6</i>	<i>BCL2</i>
DLBCL-136	<i>IGH</i>	chr16 (<i>CIITA</i> , intron 1)	chr8 (<i>TOX</i> , intron 1)	<i>BCL2</i>
DLBCL-123		<i>IGH</i> , MYC	<i>BCL6</i> , <i>IGH</i>	<i>BCL6</i> , MYC
DLBCL-154	<i>IGH</i> , <i>BCL6</i>	<i>BCL2</i> , <i>IGH</i> ; chr3 (no genes annotated)	chr12 (<i>HNRNPA1</i> , intron 1)	<i>BCL2</i> , <i>BCL6</i>
LO318	<i>IGH</i> , chr17 (~55Mb)	chr4 (~40Mb)	<i>IGH</i>	<i>BCL2</i> , MYC
DLBCL-96		<i>IGH</i>	<i>IGH</i>	<i>BCL6</i> , MYC
DLBCL-178		chr13 (<i>LCP1</i> , intron 1)	chr14 (~69Mb)	

*various targets captured by the TLC-NGS design, while the fusion partners identified are shown in the corresponding cell in each case.